



Supplement of

A dual, single detector relaxed eddy accumulation system for long-term measurement of mercury flux

S. Osterwalder et al.

Correspondence to: S. Osterwalder (stefan.osterwalder@unibas.ch)

The copyright of individual parts of the supplement might differ from the CC-BY 3.0 licence.

Table S1. Most important REA components. They are indexed in the text and in the schematic of the REA system hardware (Fig. 1) with capital letters. Devices indexed with lowercase letters are just quoted in the text.

Ind.	Qty	Component	Manufacturer	Country	Model number
A1	1	Sonic anemometer	Metek	GER	USA-1
A2	1	Sonic anemometer	Gill Instruments	UK	Solent1012R2
B	1	LabVIEW 2011	National Instruments	USA	22.6.2011
C	3	Rocker Solenoid Valves	Bürkert Fluid Control Systems	GER	6128 + 2507
D	100 m	PTFE tubing 1/4"	VICI AG International	SUI	JR-T-6810
E	3	0.2 µm PTFE filters	Merck Millipore	GER	SLFG65010
F	6	0.2 µm PTFE filters	Pall Corporation	USA	Acro 50, 4400
G	10	Teflon Isolation valves	N Research	USA	360T041
H	1	Pressure transmitter	WIKA	GER	A-10
I	3	Red-y smart controller GSC	Vögtlin Instruments	SUI	3214101
J	1	Rotary vane pump	Gardner Denver GmbH	GER	G 08
K	3	Uniplast boxes	Swibox	SUI	UCP 540/750
L	1	Dynacalibrator	VICI AG International	SUI	150
M	1	CVAFS Hg Detector	TEKRAN Inc.	CAN	2500
N	1	Swing piston vacuum pump	KNF Neuberger	GER	NPK 09 DC
O	1	Pressure gauge with water trap	Servatechnik	SUI	-
P	1	½" Hydrocarbon trap	Chromatography R.S, Inc.	USA	300
Q	20 l	Argon gas (purity>99.9997%)	Air Liquide S.A.	FRA	N57
R	1	Hg Vapor Calibration Unit	TEKRAN Inc.	CAN	2505
S	1	Digital gas-tight syringe	Hamilton	USA	1700
T	1	Hg Zero Air Generator	TEKRAN Inc.	CAN	1100

1

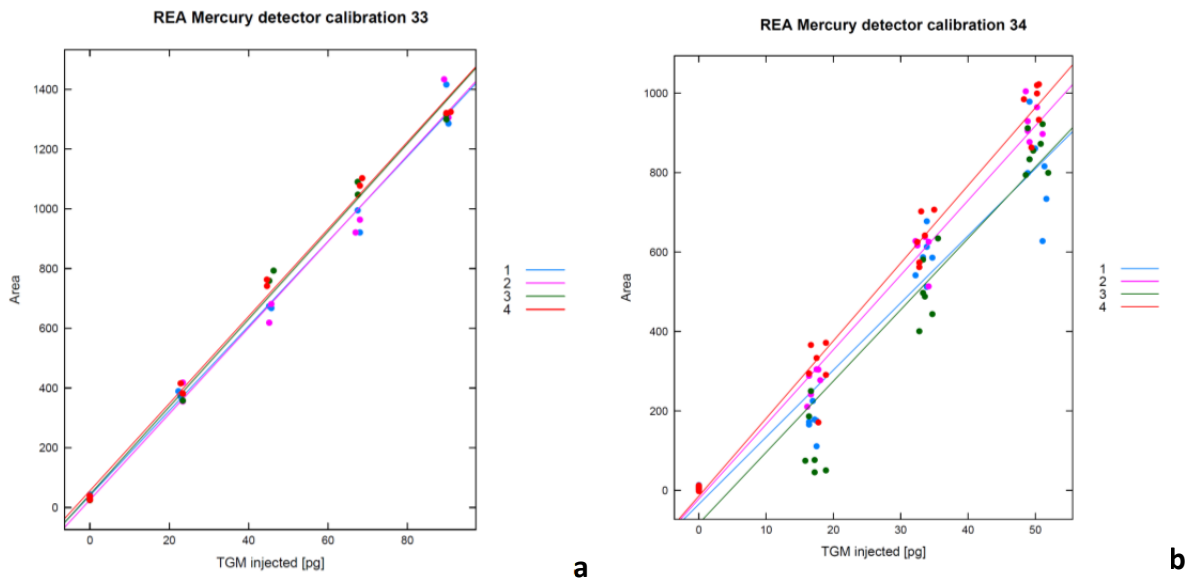


Figure S1. Linear relationship between detected GEM reference concentration on each of the four gold cartridges (1-4) and manually injected GEM [pg] for Basel (a) and Degerö (b).

2

2

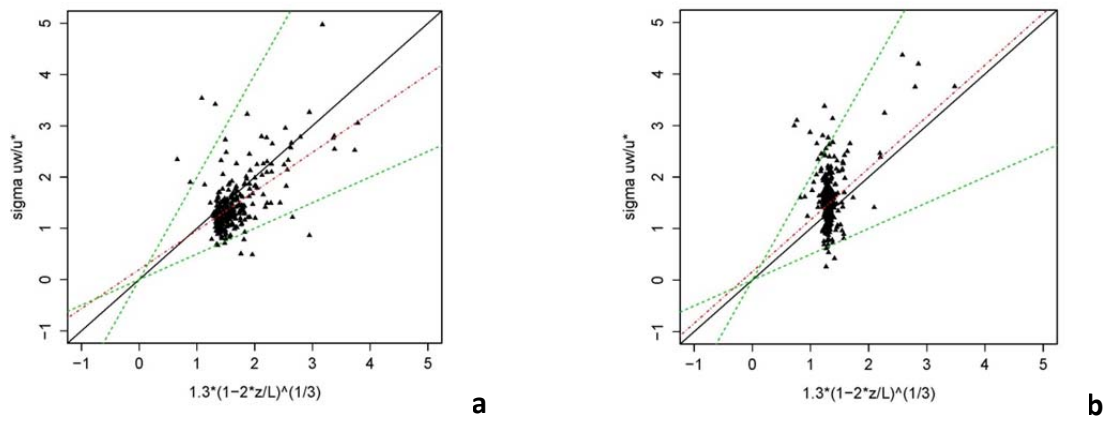


Figure S2. A factor 2 deviation from the model describing integral turbulent characteristics was used to reject data measured in Basel (a) and Degerö (b) during periods of insufficient turbulence.

3
4

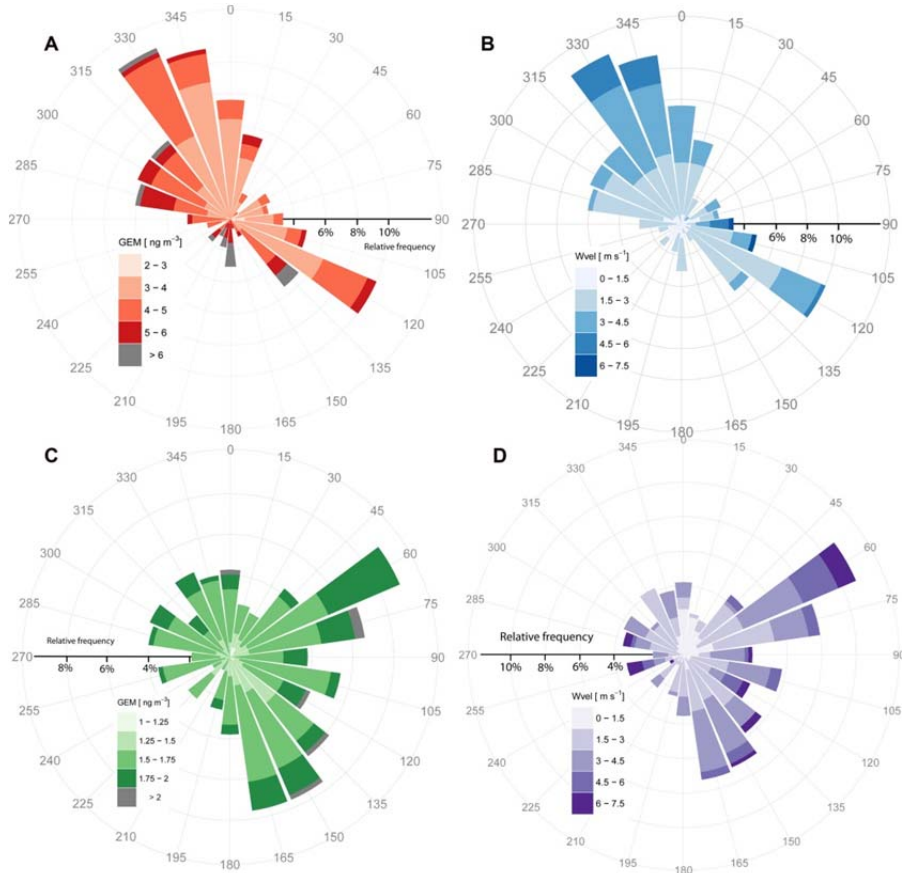


Figure S3. GEM concentration (A) and wind rose (B) during the Basel campaign and GEM concentration (C) and wind rose (D) during the Degerö campaign. Polar histograms show 30 min averaged GEM concentrations (ng m^{-3}) and wind speed (ms^{-1}).

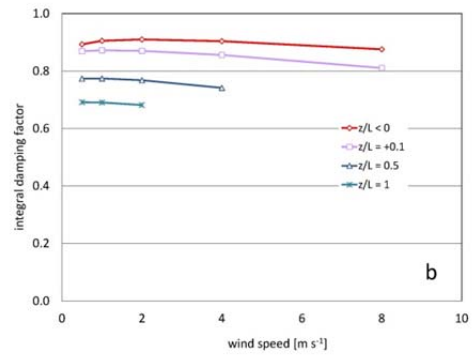
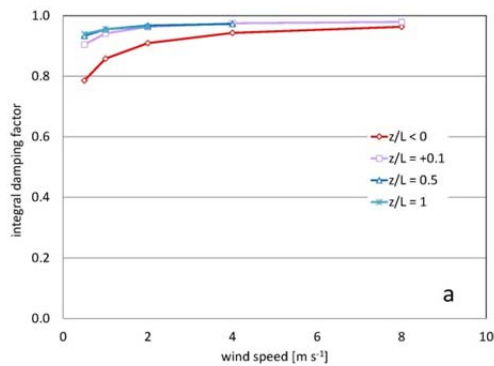


Figure S4. Simulated integral damping factors for REA fluxes in Basel (a) and Degerö (b) dependent on wind speed ($0\text{--}10 \text{ m s}^{-1}$) and stability conditions: Instable ($z/L < 0$); stable ($z/L = 0.1, z/L = 0.5, z/L = 1$).

6

7

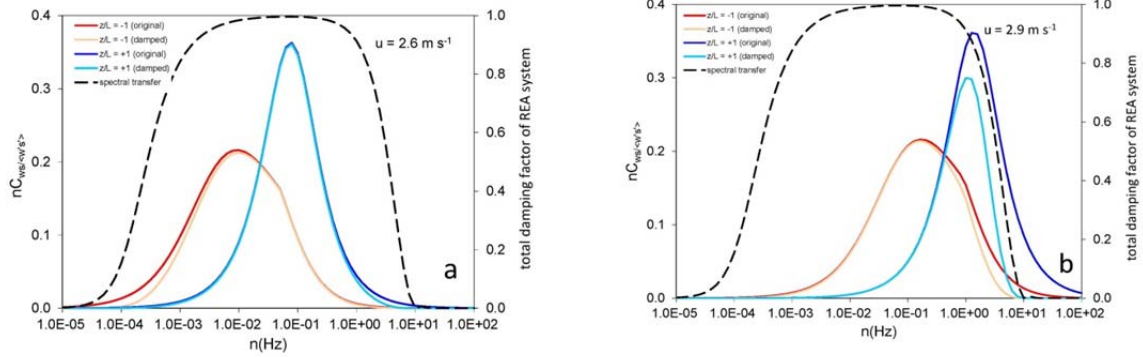


Figure S5. Modeled original and damped cospectral density and total damping factor (secondary y-axis) of REA system for Basel (a) and Degerö (b) dependent on stable ($z/L = +1$) and unstable ($z/L = -1$) conditions and mean horizontal wind speeds for both sites ($u=2.6$ and 2.9 m s^{-1} , respectively).

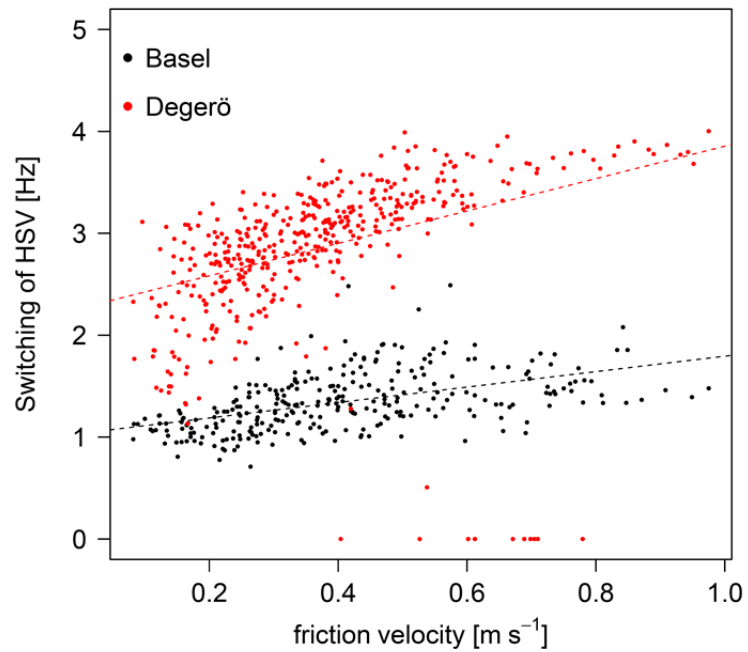


Figure S6. 30-min averaged switching frequency of fast-response valves (HSV) at Basel (black) and Degerö (red) in relation to friction velocity.